Analytical Methods

Accepted Manuscript

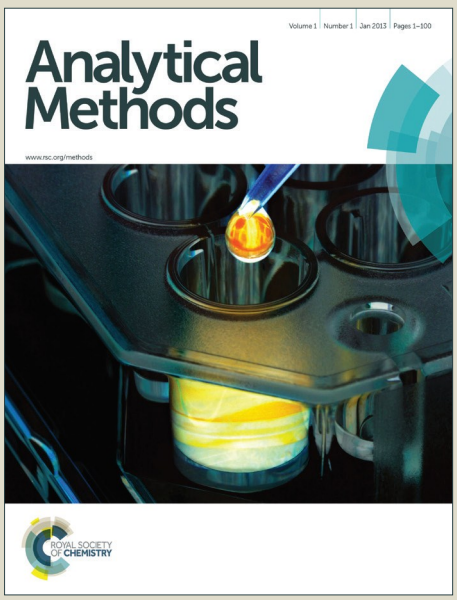

This is an *Accepted Manuscript*, which has been through the Royal Society of Chemistry peer review process and has been accepted for publication.

Accepted Manuscripts are published online shortly after acceptance, before technical editing, formatting and proof reading. Using this free service, authors can make their results available to the community, in citable form, before we publish the edited article. We will replace this *Accepted Manuscript* with the edited and formatted *Advance Article* as soon as it is available.

You can find more information about *Accepted Manuscripts* in the Information for Authors.

Please note that technical editing may introduce minor changes to the text and/or graphics, which may alter content. The journal's standard Terms & Conditions and the Ethical guidelines still apply. In no event shall the Royal Society of Chemistry be held responsible for any errors or omissions in this *Accepted Manuscript* or any consequences arising from the use of any information it contains.

ROYAL SOCIETY OF CHEMISTRY

www.rsc.org/methods

Journal Name

RSCPublishing

ARTICLE

www.rsc.org/

Anti-Stokes Raman Spectroscopy as a method to identify metallic and mixed metallic/semiconducting configurations of multi-walled carbon nanotubes

Mihaela Baibarac[a], Adelina Matea[a], Mirela Ilie[a], Ioan Baltog[a]*, Arnaud Magrez[b]

SERS studies were performed on films of two families of multi-wall carbon nanotubes (MWCNT) under an excitation light of 514.5 nm and 647.1 nm. These included Aldrich-MWCNT, which alternate semiconducting and metallic tubes and M-MWCNT that contain only metallic tubes obtained by the water assisted catalytic chemical vapour deposition (CCVD). The two families of MWCNT reveal similar spectra in the Stokes branch, which are featured by an increasing Raman intensity when the glass substrate is replaced with an Au or Ag substrate, indicating a (surface enhanced Raman scattering) SERS mechanism. In the anti-Stokes branch, despite an enhancement of approximately 100 times compared to the predictions of Boltzmann law, only the Aldrich-MWCNTs exhibit a Raman spectrum with an intensity that increases as a result of the change in the glass substrate to Au or Ag, a fact that is revealed by the signature of the SERS process. The invariance of the Raman intensity in the anti-Stokes branch as a result of the change of the substrate is a characteristic of M-MWCNT and results from a Raman light scattering process that takes place only within the skin depth of the metallic structure.

Introduction

Raman spectroscopy is one of the most commonly used techniques for characterizing and understanding the properties of carbon nanotubes[1]. The information provided using this technique are different for each type of nanotube, including single-wall carbon nanotubes (SWCNT), double-wall carbon nanotubes (DWCNT) and multi-wall carbon nanotubes (MWCNT). In the case of SWCNT, the Raman spectrum reveals three areas of interest, including one ranging from 100 to 350 cm^{-1} that contains bands associated with the radial breathing modes (RBM). Their peak position Ω is related to the tube diameter d by the relation Ω (cm^{-1}) = A/d(nm) + B, where A and B are constants for bundled, dispersed and free standing tubes [1, 2]. Bands belonging to this group are very sensitive to the excitation wavelength. The intensity of each RBM band is enhanced when the photon energy of the excitation light corresponds to a transition between the van Hove singularities (E_{ii}) in the valence and the conduction bands associated with the nanotube whose diameter is d [3]. Another group, located in the interval from 1100 to 1600 cm^{-1}, is formed from two bands, one associated with the tangential stretching modes (TM) (labelled the G band), which for the metallic nanotubes can be decomposed into Lorentzian profiles at ~1590 cm^{-1} and an asymmetric profile with a maximum at ~1540 cm^{-1}, the latter indicating an electron-phonon type interaction under an excitation energy between 1.5 – 2.2 eV [4]. In semiconducting nanotubes, the G band contains two Lorentzian profiles at ~1590 and ~1570 cm^{-1}, the former more intense than the latter [1]. The other band is frequently referred to as the "D band", whose peak position up-shifts with the energy of the laser excitation is not intrinsically related to the nanotube structure. The D band, which appears in the Raman spectrum of graphitic materials, is indicative of the disorder induced in the graphitic lattice or defects in the carbon nanotubes [1]. The third group, situated in the high frequency range from 1700-3500 cm^{-1}, corresponds to the second-order Raman spectrum. As a rule, the most intense bands are detected at approximately twice the frequency of the D and TM bands [1].

Stokes and anti-Stokes Raman scattering has been an exciting subject even in early studies of SWCNT. Much attention has been paid to the behaviour of G band and its unusual anti-Stokes Raman effect that depends on the wavelength of the exciting light. High values of the anti-Stokes/Stokes intensity ratio (I_{aS}/I_S) highlighting an anomalous intensity of the anti-Stokes emission, with regard to what Boltzmann's law states, discrepancies between the Stokes and

anti-Stokes frequencies [5-14] and different line shapes of the G band are the most distinguishing features in the anti-Stokes Raman spectra of SWCNT [5,6,9,11-14].

At thermal equilibrium, the anti-Stokes/Stokes Raman intensity ratio (I_{aS}/I_S) is established by the Boltzmann law:

$$\frac{I_{aS}}{I_S} = \left(\frac{\sigma(\alpha_\Omega)_{aS}}{\sigma(\alpha_\Omega)_S}\right)\left(\frac{\nu_l+\Omega}{\nu_l-\Omega}\right)^4 exp\left(\frac{h\Omega}{kT}\right)^{-1} \quad (1)$$

where ν_l, Ω, h, k and T are the wavenumbers of the excitation light and the Raman line (cm^{-1}), the Planck constant, the Boltzmann constant and the temperature, respectively. The terms $\sigma(\alpha_\Omega)_{aS}$ and $\sigma(\alpha_\Omega)_S$ denote the anti-Stokes and Stokes cross-sections associated with the Ω wavenumber. These terms depend on the polarizability of the material and are equal for a normal spontaneous Raman process.

The asymmetry between the Stokes and anti-Stokes spectra has generally been interpreted as resulting from a resonant Raman scattering effect produced by the excitation of different metallic *(n,m)* nanotubes [5,6]. Unfortunately this conclusion was drawn from Raman studies performed on a mixture of carbon nanotubes that was 2/3 semiconducting and 1/3 metallic as they result from synthesis procedures. At present, the success in separating SWCNT into metallic and semiconducting components, which have become commercially available [15-17], has rebooted new Raman studies to establish a distinct signature for each type of nanotube. In this context, surface enhanced Raman scattering (SERS) studies have proved to be useful for such investigations as exploiting the variation of the anti-Stokes/Stokes Raman intensity ratio *(I_{aS}/I_S)* as functions of the type of metallic support (Au, Ag) at resonant or non-resonant optical excitations for highly separated metallic and semiconducting nanotubes [18].

Focusing on the behavior of G band and using the SERS measurement technique and separate samples of SWCNT that are metallic and semiconducting with purities of 98% and 99%, respectively we have demonstrated that the enhancement of Raman intensity via a SERS effect, i.e. depending on the type of used as substrate (Au or Ag), is observed for the semiconducting nanotubes in both Raman branches, Stokes and anti-Stokes, while for the metallic nanotubes this effect is observed only in the Stokes branch. Under resonant optical excitation the occurrence of a SERS effect in the anti-Stokes Raman branch results from an over-population of the v_1 vibration level, which only exists in semiconductor nanotubes. Similarly, absence of the SERS effect in the anti-Stokes branch, even under resonant excitation of metallic nanotubes could be understood as a result of the fact that electronic levels are not refined by vibrational structure that would be overpopulated by resonant excitation [18].

Similarly, the SERS technique turned out to be a useful method to index the different structures of DWCNT including M@M, M@S, S@S and S@M where the first and second letter denote the inner and outer tube, respectively [19]. For DWCNT, the spectral range of interest is below 350 cm^{-1}, where the two Raman bands associated with the radial breathing mode (RBM) of the inner and outer tubes are located. The D and G bands are found in the range from 1100 to 1600 cm^{-1}. A feature of the G band of DWCNT is an asymmetrical profile smaller than that observed for SWNT, which is unchanged for different optical excitation energies. This is despite the fact that the inner and outer tube can be either metallic (M) or semiconducting (S), forming four possible configurations: M@M, M@S, S@M and S@S [18]. In this case, because the G band profile remains practically constant when exposed to excitation light wavelength changes or the SERS substrate, attention has focused on the RBM spectra. Using SERS with Au as a substrate and comparing the recorded anti-Stokes Raman spectra with the spectra calculated using the Boltzmann law applied to the Stokes spectra permits the observation of large differences of intensities. There are lines of the same intensity between the recorded and calculated spectrum that are associated with the metallic shell and there are lines of higher intensity in the calculated spectrum that are associated with the semiconducting shell. In this way, the RBM spectrum can be grouped into pairs of lines that are attributed to the inner and outer shells according to the M@M, M@S, S@S and S@M configurations of the DWCNT [20].

Within these results another question naturally arises, whether the same scenario for exploiting the SERS technique can be applied to establish the composition of MWCNT, i.e., if they contain metallic tubes as dominant component or an alternate metallic/semiconducting structure. The answer to this question is provided by SERS studies conducted on two types of MWCNTs, some structures consisting of semiconducting and metallic mixed coaxial tubes and other metallic structures, the latter tested by conduction measurements have been obtained by controlling the synthesis process in carpet structure that contains around 10^{11} tubes/cm^{-2} [21,22].

Experimental

In this work, measurements were performed using two types of MWCNT: a) commercial MWCNT purchased from Aldrich Sigma (Aldrich-MWCNT) and consisting of a mixed coaxial architecture alternating between metallic and semiconducting nanotubes and b) metallic MWCNT (M-MWCNT) produced in a carpet form by water assisted catalytic chemical vapor deposition (CCVD) at the Institute of Condensed Matter Physics, Lausanne (Switzerland) [20-22]. The metallic properties of the latter group were determined by the type of catalyst used in their manufacture and certified as metallic nanotubes by conduction measurements performed after purification using HCl [21-23]. Because the conduction measurements are laborious, they need to be performed on individual tubes so that may result in inconclusive statistics. In this context the question arises is whether does not could be used another experimental technique to determine the metallic or nonmetallic of MWCNTs. The answer is yes, taking into account the positive results obtained by SERS spectroscopic studies of SWCNT highly separated in metallic and semiconductor component [18]. For this purpose both types of MWCNT were dispersed in toluene under intense sonication to produce thin films that were deposited on glass and rough Ag and Au SERS supports via drop-casting to a dimension of approximately 100 nm in thickness.

The absorption spectra of the two types of MWCNT deposited on the quartz support were obtained using a UV-VIS-NIR Spectrophotometer Lambda 950 model from Perkin-Elmer.

The Raman spectroscopic studies were performed in a backscattering geometry using a T64 000 HORIBA micro-Raman system (Jobin-Yvon) equipped with a 50× focusing objective under different laser light excitation wavelengths of 514.5 nm and 647.1 nm. The laser power on the samples was 2 mW focused into a 1.2 μm^2 spot. No thermal damage effects were observed in the samples. Rough SERS supports were obtained by the thermal evaporation in a vacuum of Ag and Au onto

microscope slides using an atomic beam at a grazing angle of incidence (~80°) according to Ref. [24].

Results and discussion

This work is an extension of the SERS studies previously conducted under different optical excitation (514.5 and 676.4 nm) on SWCNT highly separated in metallic (M-SWCNT; ~98% pure) and semiconducting (S-SWCNT; ~99% pure) components depending on the type of substrate used: glass, Au or Ag [18]. We remind the reader of the main results obtained from the two cases. The main result observed on metallic nanotubes, regardless of whether resonant or non-resonant optical excitation is used with regard to the absorption spectrum, consist that the gradual increase in the G band in the Stokes branch is not accompanied by a similar variation in the anti-Stokes branch. This result is explained using a SERS mechanism that operates only in the Stokes branch. Semiconducting nanotubes exhibit a different behavior that depends on the wavelength of the excitation light when the glass support is replaced by Au or Ag. At 514.5 nm, the increase in the intensity of the Stokes branch is almost an order of magnitude higher than that of anti-Stokes branch, while at 676.4 nm, the amplification is similar between the two branches. This result reveals the signature of two enhancement mechanisms one at 514.5 nm laser excitation that occurs via surface plasmons coupling associated to the incident excitation light $SPs(\omega_l)$ and spontaneous Stokes Raman emission $SPs(\omega_l-\Omega)$, similar to a stimulated Raman effect resulting in a stronger enhancement of the Stokes Raman spectrum and another at 676.4 nm dominated by the overpopulation of the first vibrational level caused by the continuous optical pumping that takes place this explaining why the enhancement of spontaneous anti-Stokes Raman emission is larger than that provided by Boltzmann's law. In this case SERS mechanism of the whole process is revealed by the similar enhancement in the anti-Stokes and Stokes Raman emission when the glass substrate is changed to either Au or Ag [18]. A more detailed study regarding the evaluation of the effect SERS via the (I_{aS}/I_S) ratio for non-resonant or resonant optical excitation can be found in Ref.[25]

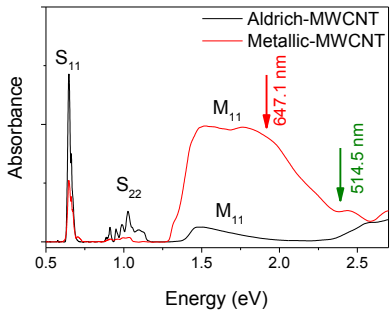

Fig. 1 Absorption spectra of the Aldrich-MWCNTs and Metallic-MWCNT obtained after baseline subtraction.

In the absorption spectrum of the Aldrich MWCNT (Fig.1 black curve) are identified S_{11} and S_{22} bands belonging semiconducting component and a band M_{11} illustrating the presence of metallic component [3]. High intensity of the band S_{11} indicates larger abundance of semiconductor components and the complex profile of the band S_{22} must be associated with the tubes of different chirality. Similarly, the absorption spectrum for metallic nanotubes (Fig.1; red curve) is dominated by an absorption band ranging 1.7-2.2 eV, which is associated with transition M_{11}. And in this case, high intensity and width of this band indicate the large number of metallic nanotubes whose chirality is different. In the red spectrum, the presence of a weaker S_{11} band should be regarded as the signature of semiconductor nanotubes present as an impurity in the assembly dominated by metallic nanotubes.

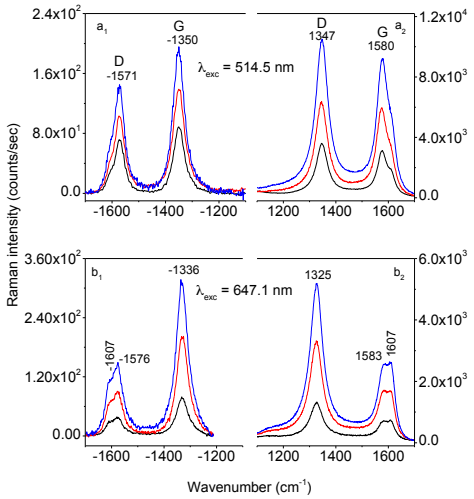

Fig. 2 Anti-Stokes (a_1;b_1) and Stokes (a_2;b_2) Raman spectra at λ_{exc} = 514.5 nm and 647.1 nm for the Aldrich-MWCNT deposited as thin films on glass (black), Au (red) and Ag (blue) supports. All spectra were recorded in a backscattering geometry with a 2 mW laser focused on the sample through a 50x objective.

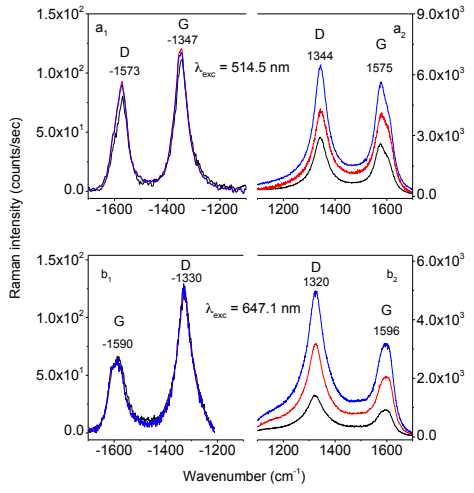

Fig. 3 Anti-Stokes (a_1;b_1) and Stokes (a_2;b_2) Raman spectra at λ_{exc} = 514.5 nm and 647.1 nm of for Metallic-MWCNT deposited as thin films on glass (black), Au (red) and Ag (blue) supports. All spectra were recorded in a backscattering geometry with a 2 mW laser focused on the sample through a 50x objective.

Let's go back to the goal in this paper to illustrate how SERS mechanism works on two types of MWCNT, some structures consisting of semiconducting and metallic mixed

coaxial tubes and other metallic structures. According to the expectations the absorption spectra of the two categories of MWCNT are different.

Figures 2 and 3 illustrate the Raman intensity variations in the Stokes and anti-Stokes branches for two excitation wavelengths, which are presumed to be resonant (647.1 nm) and non-resonant (514.5 nm) for the two types of MWCNT (those procured from Aldrich and the metallic material, respectively).

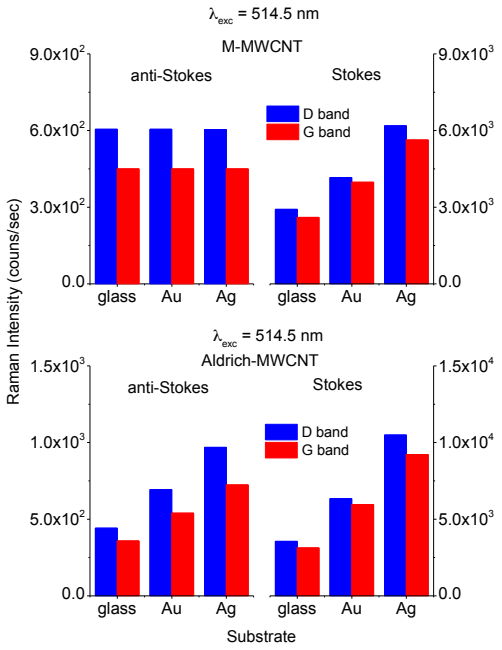

Fig. 4 Intensities of the anti-Stokes and Stokes Raman D and G lines using 514.5 nm excitation light for M-MWCNT (top) and Aldrich-MWCNT (bottom) in thin films deposited on glass, Au and Ag supports. The intensity of the laser light focused on all samples was 2 mW.

The two figures confirm the presence of G and D bands in the SERS spectra of the two types of MWCNT and highlight the different behavior in the anti-Stokes branch when the substrate is changed. These results may be more conclusive when shown in Figs. 4 and 5.

Figures 4 and 5 highlight several important details obtained from these studies: i) regardless of the wavelength of the excitation light, the Raman emission of M-MWCNT in the anti-Stokes branch is an order of magnitude smaller than for the Stokes branch, meaning that the I_{aS}/I_S ratio is higher by about two orders of magnitude compared to the predictions from the Boltzmann law; ii) regardless of the wavelength of the excitation light, the Raman emission of M-MWCNT in the anti-Stokes branch is unchanged for the G and D bands for glass Au or Ag substrate; iii) the M-MWCNT show that for the Stokes Raman branch, an increased intensity is observed (which is similar for both the G and D bands) when the substrate glass is changed with Au or Ag; iv) the Aldrich-procured MWCNT behave differently: a) both the Stokes and anti-Stokes Raman intensities increased with the change of the glass substrate using either Au or Ag and for an excitation light of 514.5 nm and 647.1 nm and b) the I_{aS}/I_S ratio is higher than the predictions from the Boltzmann law, which is similarly to that observed for M-MWCNT at 514.5 nm but three times higher for an optical excitation of 647.1 nm. What should be interpreted and understood from these results? *A priori,* the electromagnetic mechanism behind the SERS effect results from the coupling of two families of surface plasmons (SPs); one associated with the incident excitation light $SPs(\omega_l)$ and one associated with the spontaneous Raman emission that in turn are different in the Stokes $SPs(\omega_l-\Omega_i)$ and the anti-Stokes $SPs(\omega_l+\Omega_i)$ branches and are dependent on the type of metal substrate.

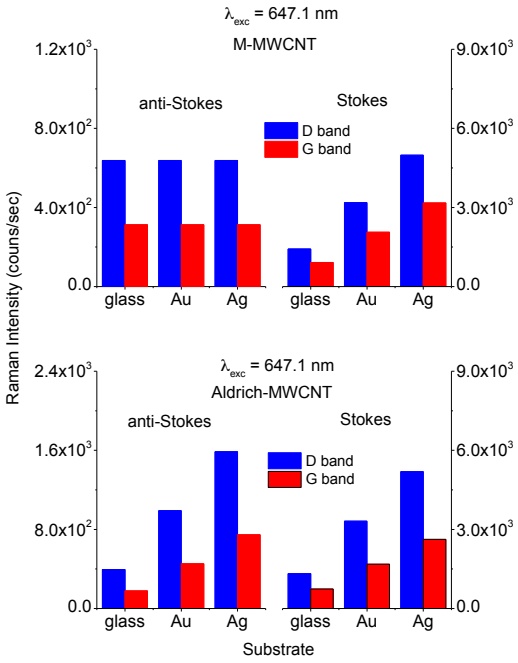

Fig. 5 Intensities of the anti-Stokes and Stokes Raman D and G lines using 647.1 nm excitation light for M-MWCNT (top) and Aldrich-MWCNT (bottom) in thin films deposited on glass, Au and Ag supports. The intensity of the laser light focused on all samples was 2 mW.

This effect is stronger for Ag than Au substrates [18, 25]. This scenario can be illustrated as follows: assume $I(\omega_l) = 1$ as the unit of intensity for the laser excitation light and consider a spontaneous Raman process in the range from 1200-1600 cm^{-1} where lines D and G are found at ~1540 cm^{-1} and ~ 1598 cm^{-1}, respectively. The intensities from the Stokes and anti-Stokes branches, the latter of which are approximated by the Boltzmann law, are approximately $I(\omega_l-\Omega_i) \approx 10^{-6}$ and $I(\omega_l+\Omega_i) \approx 10^{-9}$, respectively. As shown, these intensities differ by an order of magnitude, and these differences are maintained between the evanescent waves that are associated with the corresponding plasmons so that $SPs(\omega_l) >> SPs(\omega_l-\Omega_i) >> SPs(\omega_l+\Omega_i)$. The variable Ω_i was observed to determine the Raman shifts associated with the G or D Raman lines. In these circumstances, it is obvious that the coupling $SPs(\omega_l) \rightarrow SPs(\omega_l-\Omega_i)$ is more efficient than the coupling $SPs(\omega_l) \rightarrow SPs(\omega_l+\Omega_i)$, which explains the stronger enhancement in the Stokes branch than in the anti-Stokes branch, which acts as a supplementary fingerprint for the SERS effect, depending on the type of metallic substrate. Such a process is quite similar to the generation of a stimulated Raman emission caused by the mixing of two surface evanescent

waves separated by a Raman frequency Ω_i [25]. Returning to the anti-Stokes Raman spectra of the two types of MWCNT, this explanation requires examination in greater detail.

For the Aldrich sample, the anti-Stokes spectra leads to a I_{aS}/I_S ratio that is higher by ~100 times compared to the predicted results from the Boltzmann law. Additionally, a SERS effect is noticed by the variation of this ratio depending on the type of metallic substrate used (either Au or Ag). The higher value of the I_{aS}/I_S ratio bears the imprint of a resonant optical excitation process associated with the presence of semiconductor nanotubes in the MWCNT architecture, which is even stronger for a 647.1 nm excitation light, which causes the value of the I_{aS}/I_S ratio to increase up to ~300. As was demonstrated in Ref. [18], such a result is a consequence of an overpopulation in the first vibrational level of the semiconducting component from the MWCNT architecture obtained under continuous optical excitation and inducing an enhancement in the anti-Stokes emission, even in the absence of the SERS effect.

For M-MWCNT, the Stokes branch displays a variation in the Raman intensity that is typical for the SERS process, i.e., a supplementary enhancement is observed when an Au substrate is replaced with an Ag substrate. Additionally, the ratio I_{aS}/I_S increases by ~100 times over what is predicted by the Boltzmann law. This actually indicates a resonant optical excitation, which causes a lack of intensity variation in the anti-Stokes Raman branch when changing the substrate, requiring a more subtle evaluation of the entire Raman scattering process.

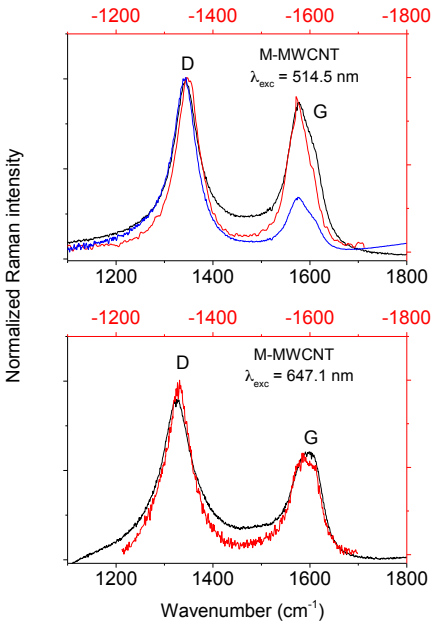

Fig. 6 Normalized profile of the D and G bands in the Stokes (black curves) and the anti-Stokes (red curves) branch of M-MWCNT at two excitation laser light wavelengths. The blue curve shows the normalized profile of calculated anti-Stokes spectrum from the Boltzmann law.

To fully address this issue, we need to examine the metallic nature of the sample and the peculiarities of a Raman process. It is known that the intensities of Raman lines in metals are very small because the light scattering process takes place only within the skin depth, to which is added the large impedance mismatch between the metal and the air that governs a small efficiency for the energy transfer into and out of the metal sample [26]. The mechanism for Raman scattering originates in the modulation of electric susceptibilities $\chi(\Omega_i)$ by optical vibration modes within the skin depth, as seen for M-MWCNT, which could explain the occurrence of a resonant Raman effect noticed by a higher value (more than ~100 times) in the I_{aS}/I_S ratio compared to the Boltzmann law predictions, as shown in Figure 3. If such an explanation is valid for the invariance in the anti-Stokes Raman intensity despite changing the substrate, it remains to be seen why the Raman intensity increases in the Stokes branch when the glass substrate is replaced with either Au or Ag. For this, we must consider the above scenario to explain the SERS effect that occurs in the case of Aldrich-MWCNT, which involve a transfer of energy from the excitation light towards the Stokes branch via the coupling of corresponding surface plasmons. The increase in the Stokes Raman intensity with the change in the glass substrate to Au or Ag results from a higher excitation intensity provided by a confinement effect of the electromagnetic field at the Au/air and Ag/air interfaces, which is stronger for the latter case. Finally, to all of these explanations must be added another argument including that the high value of the I_{aS}/I_S ratio cannot be the result of an uncontrolled thermal effect, which is a highly effective leading to the enhancing the anti-Stokes emission. This is seen in Figure 6, which shows that on a normalized scale the profiles of the D and G bands in Stokes and anti-Stokes branches remain unchanged.

A thermal effect should lead to changes in the profile of the anti-Stokes branch and a relative change in the intensities of G and D bands, which is not observed. A profile change and the change of the ratio between the intensities of the D and G lines by simply transcribing the Boltzmann law of a Stokes spectrum in an anti-Stokes spectrum is shown in the blue curve of Figure 6.

Conclusions

In this paper, we have performed systematic SERS studies under different excitation light conditions on films containing two families of MWCNT, namely Aldrich-MWCNT, containing alternating of semiconducting and metallic tubes and M-MWCNT containing only metallic tubes. The major results are as follows:

i) For the Stokes branch, both types of nanotubes show Raman spectra that increase in intensity with a change of the glass substrate to Au and Ag. This enhancement proves that a SERS mechanism with an electromagnetic origin consisting of the coupling of plasmons is associated with the incident excitation light and spontaneous Stokes Raman scattering.

ii) In the anti-Stokes Raman range, regardless the wavelength of the excitation light, both types of nanotubes exhibit a Raman intensity of approximately ~100 times higher than the predictions from the Boltzmann law. This result indicates a resonant optical excitation that occurs both in the Aldrich-MWCNT and M-MWCNT.

iii) In the anti-Stokes Raman range, only the Aldrich-MWCNT exhibit an enhancement in the Raman intensity with a change in the glass substrate to Au and Ag and indicate a SERS mechanism.

iv) The invariance of the SERS intensity in the anti-Stokes branch to a change in the substrate is a characteristic of M-

MWCNT, and results from a Raman light scattering process that takes place only within the skin depth of the metallic structure. In this context SERS spectroscopy in anti-Stokes branch can be considered a useful method for identifying of metallic or metallic-semiconductor mixture of MWCNT, often imposed requirement in the preparation of composites for various applications. However, we should mention that due to the shielding effect played of metallic nanotubes, the data presented here cannot establish unambiguously whether invariance of the SERS spectra in the anti-Stokes branch to the change of the substrate result only from signature of outer nanotube or it actually reflects the global nature of the whole architecture of MWCNT.

Acknowledgments

This work was funded by the Romanian National Authority for Scientific Research, CNCS-UEFISCDI, project PN-II-ID-PCE-2011-3-0619 and the Swiss National Science Foundation – Switzerland, project SCOPES number I74Z0_137458.

Notes and references

[a]National Institute of Materials Physics, P.O. Box MG-7, 077125 Bucharest-Magurele, E-mail: ibaltog@infim.ro (I. Baltog) Tel (office): + 40 21 3690170; Fax (office): + 40 21 3690177.
[b]Ecole Polytechnique Fédérale Lausanne, Institute of Condensed Matter Physics, CH-1015 Lausanne, Switzerland.

1 A. Jorio, M. S. Dresselhaus and G. Dresselhaus, *Carbon Nanotubes (Topics in Applied Physics*), Springer-Verlag Berlin, Heidelberg, 2008, vol.111.
2 S. M. Bachilo, M. S. Strano, C. Kittrell, R. H. Hauge, R. E. Smalley, and R. B. Weisman, *Science*, 2002, **298**, 2361-2366.
3 H. Kataura, Y. Kumazawa, Y. Maniwa, I. Umezu, S. Suzuki, Y. Ohtsuka, and Y. Achiba, *Synthetic. Met.,* 1999, **103**, 2555-2558.
4 M. A. Pimenta, A. Marucci, S. A. Empedocles, M. G. Bawendi, E. B. Hanlon, A. M. Rao, P. C. Eklund, R. E. Smalley, G. Dresselhaus, and M. S. Dresselhaus, *Phys. Rev. B*, 1998, **58,** R16016-R16019.
5 K. Kneipp, H. Kneipp, P. Corio, S. D. M. Brown, K. Shafer, J. Motz, L. T. Perelman, E. B. Hanlon, A. Marucci, G. Dresselhaus, and M. S. Dresselhaus, *Phys. Rev. Lett*., 2000, **84**, 3470-3473.
6 S. D. M. Brown, P. Corio, A. Marucci, M. S. Dresselhaus, M. A. Pimenta, and K. Kneipp, *Phys. Rev. B*, 2000, **61**, R5137-R5140.
7 P. V. Teredesai, A. K. Sood, A. Govindaraj, and C. N. R. Rao, *Appl. Surf. Sci.*, 2001, **182**, 196-201.
8 A. G. Souza Filho, A. Jorio, J. H. Hafner, C. M. Lieber, R. Saito, M. A. Pimenta, G. Dresselhaus, and M. S. Dresselhaus, *Phys. Rev. B,* 2001, **63**, 241404(R).
9 S. L. Zhang, X. Hu, H. Li, Z. Shi, K. T. Yue, J. Zi, Z. Gu, X. Wu, Z. Lian, Y. Zhan, F. Huang, L. Zhou, Y. Zhang, and S. Iijima, *Phys. Rev. B*, 2002, **66**, 035413.
10 P. H. Tan, L. An, L. Q. Liu, Z. X. Guo, R. Czerw, D. L. Carroll, P. M. Ajayan, N. Zhang, and H. L. Guo, *Phys. Rev. B*, 2002, **66**, 245410.
11 V. Zolyomi, and J. Kurti, *Phys. Rev. B*, 2002, **66**, 073418.
12 L. G. Cançado, M. A. Pimenta, R. Saito, A. Jorio, L. O. Ladeira, A. Grueneis, A. G. Souza-Filho, G. Dresselhaus, and M. S. Dresselhaus, *Phys. Rev. B,* 2002, **66**, 035415.
13 A. G. Souza Filho, S. G. Chou, Ge. G. Samsonidze, G. Dresselhaus, M. S. Dresselhaus, L. An, J. Liu, A. K. Swan, M. S. Ünlü, B. B. Goldberg, A. Jorio, A. Grüneis, and R. Saito, *Phys. Rev. B*, 2004, **69**, 115428.
14 I. Baltog, M. Baibarac, and S. Lefrant, *Phys. Rev. B,* 2005, **72**, 245402.
15 R. Krupke, F. Hennrich, H. von Lohneysen, and M. M. Kappes, *Science*, 2003, **301**, 344-347.
16 S. Banerjee, T. Hemraj-Benny, and S. S. Wong, *J. Nanosci. Nanotechnol.,* 2005, **5**, 841-855.
17 G. F. Lin, L. J. Meng, X. K. Zhang, and Q. H. Lu, *Prog. Chem.*, 2010, **22**, 331-337.
18 M. Baibarac, I. Baltog, L. Mihut, and S. Lefrant, *J. Raman. Spectrosc.* 2014, **45**, 323-331.
19 P. Rudolf, P. Thomas, A. K. Yoong, and K. Hans, Double-wall carbon nanotubes. In *Carbon Nanotubes (Topics in Applied Physics)*, ed A. Jorio, M. S. Dresselhaus, G. Dresselhaus, Springer-Verlag Berlin, Heidelberg, 2008, vol.111, pp. 495-530.
20 M. Baibarac, I. Baltog, A. Matea, L. Mihut, and S. Lefrant, *J. Raman. Spectrosc*., 2014, **46**, 32-38.
21 R. Smajda, J. C. Andresen, M. Duchamp, R. Meunier, S. Casimirius, K. Hernadi, L. Forro, and A. Magrez, *Phys. Status. Solidi B*, 2009, **246**, 2457-2460.
22 A. Magrez, J. W. Seo, R. Smajda, M. Mionic, and L. Forro, *Materials,* 2010, **3**, 4871-4891.
23 R. Sanjines, M. D. Abad, Cr. Vaju, M. Mionic, and A. Magrez, *Surf. Coat. Tech.*, 2011, **206**, 727-733.
24 S. Lefrant, I. Baltog, and M. Baibarac, *J. Raman. Spectrosc.,* 2005, **36**, 676–698.
25 M. Baibarac, I. Baltog, L. Mihut, A. Matea, and S. Lefrant, *J. Optics*, 2014, **16**, 035003.
26 D. L. Mills, and A. A. Maradudin, *Ann. Phys.-New York*, 1970, **56**, 504-555.

